AMD - Vol. 55

# Rotor Dynamical Instability

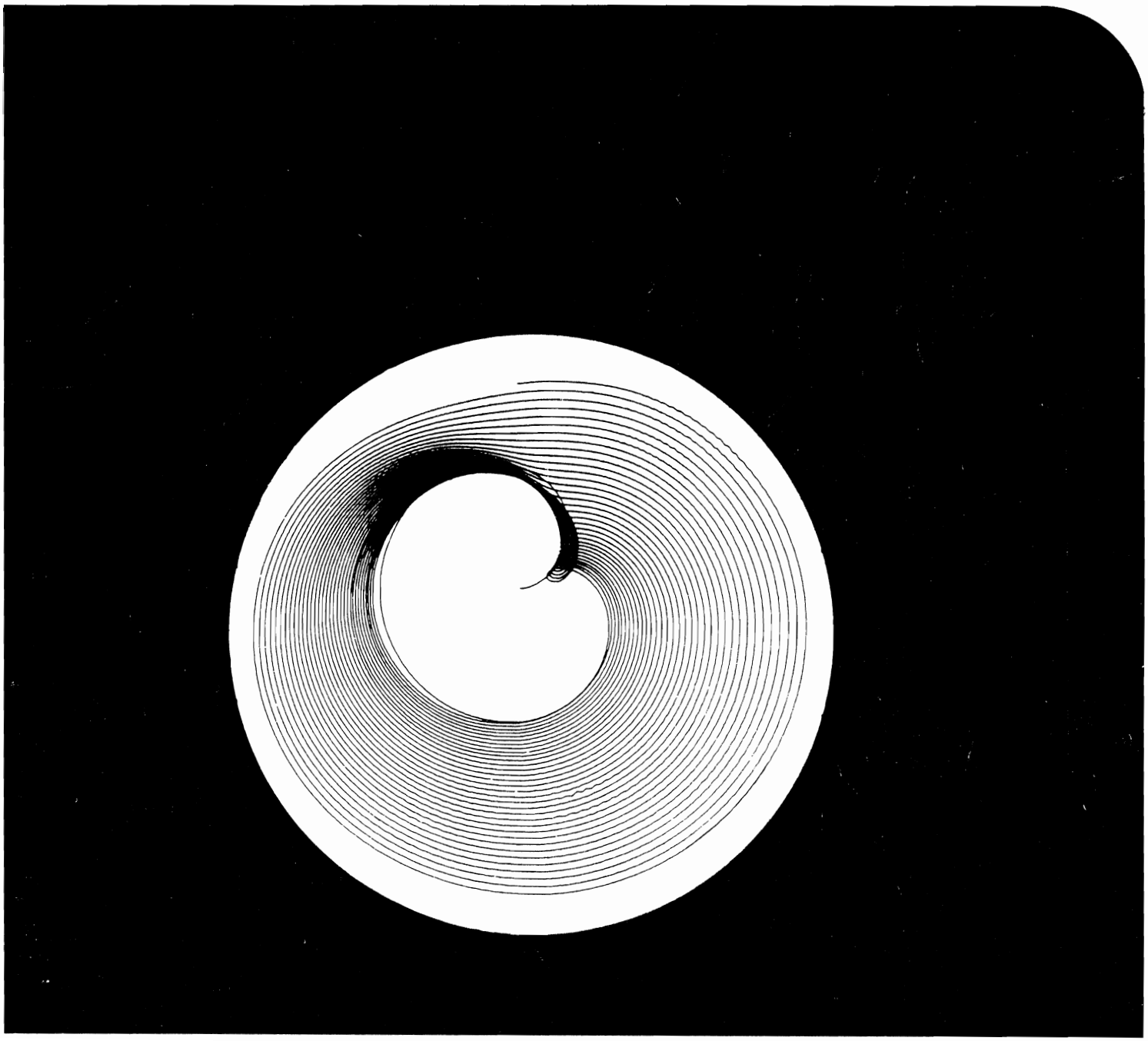

AMD - Vol. 55

# Rotor Dynamical Instability

*presented at*

THE APPLIED MECHANICS, BIOENGINEERING,
AND FLUIDS ENGINEERING CONFERENCE
HOUSTON, TEXAS
JUNE 20-22, 1983

*sponsored by*

APPLIED MECHANICS DIVISION, ASME

*edited by*

MAURICE L. ADAMS, JR.
CASE WESTERN RESERVE UNIVERSITY

THE AMERICAN SOCIETY OF MECHANICAL ENGINEERS

# INFLUENCE OF UNBALANCE ON THE NONLINEAR DYNAMICAL RESPONSE AND STABILITY OF FLEXIBLE ROTOR-BEARING SYSTEMS

**E. J. Gunter and R. R. Humphris**
Department of Mechanical and Aerospace Engineering
University of Virginia
School of Engineering and Applied Science
Charlottesville, Virginia

**H. Springer**
Institut fuer Maschinendynamik
Wien, Austria

ABSTRACT

In this paper, some of the effects of unbalance on the nonlinear response and stability of flexible rotor-bearing systems is presented from both a theoretical and experimental standpoint. In a linear system, operating above its stability threshold, the amplitude of motion grows exponentially with time and the orbits become unbounded. In an actual system, this is not necessarily the case. The actual amplitudes of motion may be bounded due to various nonlinear effects in the system. These nonlinear effects cause limit cycles of motion. Nonlinear effects are inherent in fluid film bearings and seals. Other contributors to nonlinear effects are shafts, couplings and foundations. In addition to affecting the threshold of stability, the nonlinear effects can cause jump phenomena to occur at not only the critical speeds, but also at stability onset or restabilization speeds.

INTRODUCTION

This paper presents some of the effects of unbalance on the nonlinear response and stability of flexible rotor-bearing systems. In the analysis of the stability of rotor-bearing systems, the system is analyzed from the standpoint of a linearized spring-mass damping system. In the linear sense, the threshold of stability is determined from the characteristics of the damped eigenvalues. When the real component of a damped eigenvalue becomes positive, the system is said to be unstable in the linear analysis.

In a linear system, operating above its stability threshold, the amplitude of motion grows exponentially with time and the orbits become unbounded. In an actual system, this is not necessarily the case. The actual amplitudes of motion may be bounded due to various nonlinear effects in the system. These nonlinear effects cause limit cycles of motion.

Hydrodynamic fluid film bearings exhibit highly nonlinear characteristics. The standard practice for dynamic unbalance response and stability analysis is to determine the linearized bearing stiffness and damping coefficients about a steady state equilibrium position. This for example results in 8 stiffness and damping coefficients to describe the hydrodynamic bearing characteristics for a given steady state Summerfeld number. In this mathematical assumption, the rotor is exhibiting small displacements about the equilibrium position.

In the case of low values of unbalance, the synchronous motion about the

steady state equilibrium position is described by ellipses. However, when the unbalance level becomes moderate to large, the rotor orbits are not necessarily elliptical, due to the highly nonlinear characteristics of the fluid film. Under moderate to large values of unbalance, the rotor stability characteristics are also greatly affected in both rigid and flexible rotors. The influence of large values of unbalance must also be considered in the design of squeeze film dampers, which are closely related in characteristics to journal bearings. Proper design of squeeze film dampers for example cannot be performed without taking into consideration the highly nonlinear characteristics of the damper.

In addition to affecting the threshold of stability, the nonlinear effects can cause jump phenomena to occur at the critical speeds. The nonlinear jump is caused by the equivalent or effective hardening spring rate of the journal bearing. In practice, when the synchronous jump-down in amplitude occurs, the reduction in synchronous loading often causes a nonsynchronous motion in the system. Therefore, the high nonsynchronous whirl motion may be associated with low levels of unbalance. Under some circumstances, a lower total level of vibration of motion may be obtained by having a moderate level of rotor unbalance in the system. This is because a well balanced rotor may exhibit large nonsynchronous motion at the high operating speed. In the case of the large to moderate levels of unbalance, the rotating unbalance load stabilizes the rotor system.

An interesting illustration of this phenomena is found in vertical water pumps with plain journal bearings. In the case where the rotor is well balanced, the rotor is inherently unstable. However, if a moderate level of unbalance is placed upon the rotor, then the rotor may operate without self-excited instability. The ability to do this is also dependent upon the ambient pressure in the bearing, as the cavitation conditions affect the phenomena of self-excited instability.

The analysis of the nonlinear effects in rotor-bearing systems is extremely difficult and there are few analytical procedures that will generate valid results over a wide range of parameters. The most commonly accepted method for nonlinear analysis is to perform a time-transient numerical integration of the complete equations of motion. Therefore, even for relatively simple systems, this becomes a formidable task since the Reynolds' equation must be evaluated at each time step. Time-transient studies have been effectively performed, using both the digital and analog computers by numerous investigators, such as Castelli, Rieger, Gunter, Kirk, Childs, Choy, Li, Barrett and Nelson.

In the case of nonlinear rotor-bearing dynamics, each situation must be analyzed on its own merits. It is difficult to formulate general design rules, as is the case for linearized rotor-bearing systems.

In this paper, some of the nonlinear characteristics of fluid film journal bearings will be described along with experimental data for rigid and flexible rotor-bearing systems.

## NONLINEAR RIGID JOURNAL BEARING MOTION

Fig. 1 represents a shaft in a plain journal bearing for a rigid rotor with cylindrical motion only. This system has two degrees of freedom. If the journal bearing is mounted upon a flexible support, which would represent foundation effects, then 2 additional degrees of freedom are introduced into the system. The analysis of the fluid film is given by the well known Reynolds' equation and has been extensively investigated by many authors.

A typical hydrodynamic pressure profile generated in the plain bearing is shown in Fig. 2. The integration of the hydrodynamic pressure profile produces the nonlinear forces acting upon the journal bearing. The integration of the perturbed bearing pressure, due to small displacements, generates the 8 characteristic bearing stiffness and damping coefficients used in linear analysis. An extensive study of the plain journal bearing has been done by Badgley and Booker, Kirk, Gunter, Holmes, Lund and other investigators.

In order to examine the nonlinear characteristics of a journal bearing, it is necessary to numerically integrate the dynamical equations of motion forward in time. In this procedure, the bearing pressure profile is integrated to determine the forces acting upon the shaft and the resulting motion is determined by various numerical procedures, such as Runga-Kutta or the Newmark-Beta method.

In the example shown in Fig. 3, a horizontal balanced rotor is released from the origin and precesses about in a decreasing spiral until it reaches the stable eccentricity position of ES=0.21. In this case, the rotor is operating just below the threshold of stability. After each cycle of shaft motion, a timing reference mark is placed on the orbit. From observation of the location of the timing marks on the orbit, it can be seen that the orbital motion is approximately half-frequency whirl. After about 10 cycles of motion, the shaft reaches its steady-state equilibrium position.

Fig. 4 is similar to Fig. 3, except that a rotating unbalance of 60 lbs has been added to the shaft. The unbalance eccentricity EMU is 20% of the bearing clearance. In this case, the rotating unbalance load produces a characteristic internal loop which is an indication that subsynchronous whirl is present in the system. This characteristic inside loop cannot be obtained by a linearized analysis.

A vector combination of synchronous and half-frequency whirl motion is shown in Fig. 5. When the motion is all synchronous, as shown in the upper left hand figure, the orbit is circular or elliptical and has only one timing mark on it. When half-frequency whirl motion is present in the system, the orbit appears to have an inner loop. As the magnitude of the half-frequency whirl component increases in relationship to the synchronous component, the size of the internal loop reduces. When the half-frequency whirl for example is 70% of the total motion, there is no characteristic internal loop but only a cusp. When the subsynchronous component is over 80% of the total motion, then the orbit appears circular with two timing marks appearing on the orbit.

Fig. 6 represents the rotor, as shown in Fig. 4, except that the rotor speed has been increased to 10,500 RPM. In this case, the rotor is operating well above the stability threshold which is approximately 6500 RPM. After two cycles of shaft motion, it can be seen from an approximate analysis of the size of the inside loop, that the subsynchronous motion is 60% of the total motion. After two more cycles, a cusp is formed indicating that the subsynchronous motion is now 70% of the total motion. After ten more cycles of shaft motion however the rotor amplitude does not continue to increase, but forms a limit cycle in which approximately 85% of the bearing clearance is taken up. This finite amplitude or limit cycle is due to the nonlinear forces of the journal bearing.

A comparison of rotor half-frequency whirl motion at the threshold of stability for linear and nonlinear bearings is illustrated in Fig. 7, with Fig. 7A representing the linear motion for 20 cycles. It is noted that the amplitude grows or becomes unbounded with time for this linear system. Fig. 7B shows that with a nonlinear system, a finite limit cycle is present. The nonsynchronous component remains bounded. It is for this reason that rotor-bearing systems are often able to operate substantially above their threshold of stability. Also, various hydrodynamic bearing types will exhibit distinctly different limit cycle characteristics.

The rotor system as shown in Fig. 8 is similar to Fig. 6, with operation at 10,500 RPM, except that the unbalance has been increased from EMU=.2 to 0.8. In a linear system, for example, the amount of the forcing function does not affect the characteristics of the system. The magnitude of the response is changed linearly. From Fig. 8 it can be seen that there is a dramatic change in the nature of the orbit. The motion has been completely changed to synchronous precession with no indication of self-excited whirl motion. The rotating load, FU, on the system for EMU=.8 is 625 lb. The dynamic transmissibility, TRD, for this bearing is 1.67 and therefore the maximum forces transmitted through the bearing is larger than the rotating unbalance load. This is not necessarily considered a satisfactory design. Thus, from the standpoint of forces transmitted, it is not necessarily a desirable design procedure to apply large rotating unbalance loads in order to stabilize a journal bearing at high speed. One must also consider the dynamic transmissibility of the system. Again, it should be noted that the dynamic transmissibility for large rotating unbalance loads cannot be calculated by normal linearized theories. For example, for conventional theory we assume small pertubations about the journal equilibrium position. In this case, it is observed that there is a large orbiting occurring about the journal center. Linearized theory is not applicable in this case.

Shown in Fig. 9 are the orbits of a journal bearing obtained with four

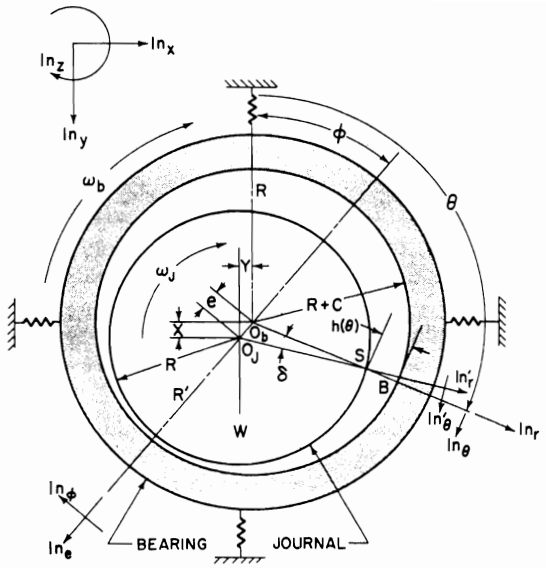


Fig.1 Plain journal bearing on flexible supports

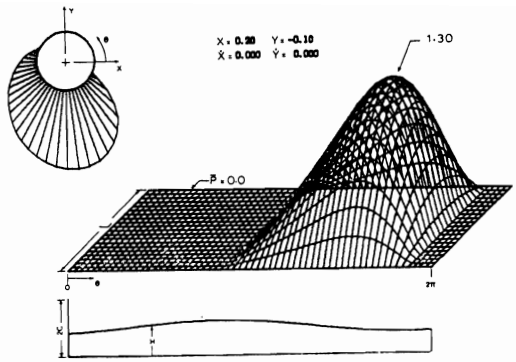

Fig.2 Hydrodynamic pressure profile with idealized cavitation

N = 6500 RPM
R = 1.00 IN.
L = 1.00 IN.
C = 5.00 MILS
TRSMAX = 1.29
S = 1.733
SS = 0.433

WT = 1.00
W = 50 LB.
MU*5 = 1.000 REYNS
FMAX = 64.4 LB. AND
OCCURS AT 0.53 CYCLE
WS = 2.45
ES = 0.211

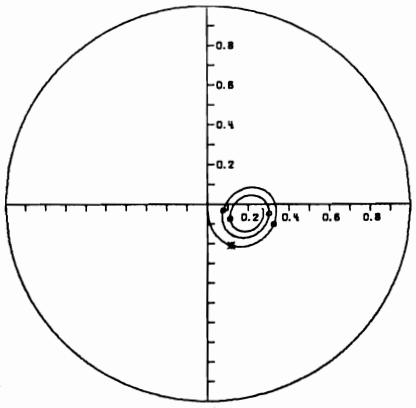

Fig.3 Journal bearing orbit of a balanced horizontal rotor

N = 6500 RPM
R = 1.00 IN.
L = 1.00 IN.
C = 5.00 MILS
TRSMAX = 2.66
S = 1.733
SS = 0.433
EMU = 0.20
SU = 1.446
TRDMAX = 2.22

WT = 1.00
W = 50 LB.
MU*5 = 1.000 REYNS
FMAX = 133.0 LB. AND
OCCURS AT 0.86 CYCLE
WS = 2.45
ES = 0.211
FU = 59.95 LB.
FURATIO = 1.20
ESU = 0.244

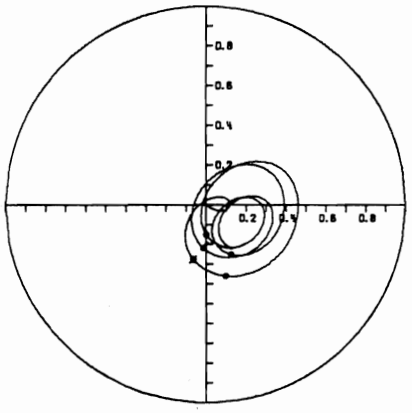

Fig.4 Journal bearing orbit of an unbalanced horizontal rotor at the stability threshold for 5 cycles

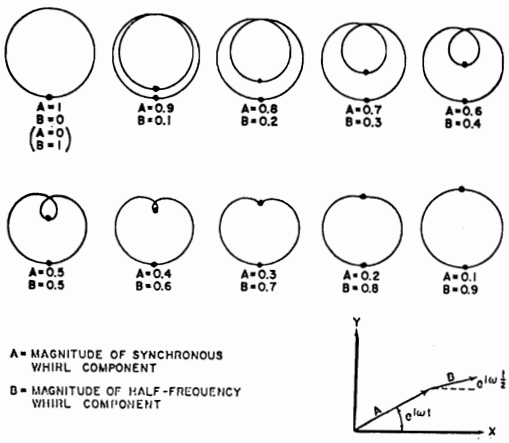


Fig.5 Orbit combinations of synchronous and half-frequency whirl

N = 10500 RPM
R = 1.00 IN.
L = 1.00 IN.
C = 5.00 MILS
TRSMAX = 4.97
S = 2.800
SS = 0.700
EMU = 0.20
SU = 0.895
TRDMAX = 1.59

WT = 1.00
W = 50 LB.
MU*5 = 1.000 REYNS
FMAX = 248.7 LB. AND
OCCURS AT 8.95 CYCLE
WS = 3.96
ES = 0.139
FU = 156.45 LB.
FURATIO = 3.13
ESU = 0.342

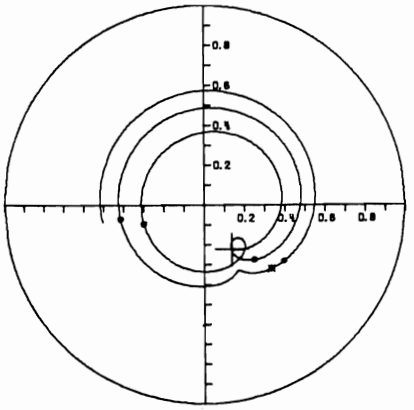

Fig.6 Journal bearing orbit of an unbalanced horizontal rotor above the stability threshold for cycles 5-10

different values of unbalance with the rotor operating above its linear threshold speed. For case 1 with EMU=.2, it can be seen that the subsynchronous component is approximately 70% of the total orbit by comparing this figure with Fig. 5. As the unbalance eccentricity is increased from .2 to .22, the size of the inside loop increases, indicating that the subsynchronous component has reduced to 50 to 60% of the total orbit. A further increase in unbalance to EMU= 0.25 reduces the subsynchronous component to approximately 20% of the total orbit. A further slight increase of the unbalance eccentricity to EMU=0.26 causes a complete stabilization of the rotor orbit. It is also of interest to note that the dynamic transmissibility for EMU=0.2 is TRD=1.35. The increase of unbalance to EMU=0.26 causes the dynamic transmissibility to reduce to 1.02. Therefore, in this case, it is seen that it is desirable to have an unbalance eccentricity of approximately 26% of the bearing clearance when operating above the stability threshold for this particular case.

In addition to affecting the rotor stability threshold, the amount of unbalance in the journal affects the center of the orbit and the size and shape of the orbit due to the nonlinear characteristics of the bearing. Fig. 10 represents the synchronous whirl orbits obtained for a steady state load with dimensionless values of unbalance ranging from .1 to EMU=1.0. In the case of EMU= 0.1, the system can be accurately described by linearized bearing theory. As the unbalance increases from .1 to 0.4, it is seen that the orbit is no longer elliptical. The lower portion of the orbit follows closely the journal profile. A set of pseudo stiffness and damping coefficients may be used to approximate the journal orbit by means of an energy approach. It is seen that in this case the center of the orbit or the apparent bearing equilibrium position has shifted from the steady state value towards a position that appears to become more and more centered in the journal bearing. Further research needs to be performed in this area of determining the effective bearing stiffness and damping characteristics for large values of unbalance and orbits that are not elliptical.

The onset of instability and also the magnitude of the bearing limit cycle is affected by the oil supply and the ambient pressure of the bearing. For example, Fig. 11 represents an idealized uncavitated bearing pressure profile. Normally, the high negative pressure as shown in Fig. 11 does not occur and the film ruptures. This ruptured film is referred to as a cavitated film with a collapse of the pressure profile in the cavitation region. However, under certain circumstances, such as with seals or vertical water pumps under high pressures, the pressure profile as shown in Fig. 11 can exist. If no cavitation is permitted in the bearing, then the plain journal bearing is inherently unstable under all operating conditions. The ambient pressure level will determine when cavitation in the film occurs.

The limit cycle orbits obtained with various ambient pressure levels for the rotor operating at 10,500 RPM with rotor unbalance are given in Fig. 12. With the original amount of unbalance, the rotor is stable with 0 ambient pressure levels. As the pressure level is increased from 0 to 100 psi, subsynchronous motion occurs. A further increase of ambient pressure to 1,000 psi causes a large subsynchronous limit cycle to occur which occupies over 70% of the bearing clearance. If plain journal bearings, for example, are used in high pressure vertical water pumps, then large limit cycle motion may be expected. This would cause bearing and seal wearing to occur with an eventual increasing of the pump seal leakage rates. Plain bearings should be avoided in such circumstances.

## NONLINEAR FLEXIBLE ROTOR-BEARING MOTION AND STABILITY

### Theoretical Computer Simulations

A single mass Jeffcott rotor mounted in journal bearings on inflexible supports is shown in Fig. 13. In this system, nonlinear effects can arise from the rotor, as well as the journal bearings and the support system. Under high vibrational amplitudes, the bearing characteristics may not be assumed to act at a planar location. The ends of the bearings act to decrease the effective shaft length producing nonlinear shaft stiffness effects.

Fig. 14 represents the unbalance response characteristics for the Jeffcott rotor assuming linear bearings and shaft characteristics. This figure gives the response curve for various values of assumed rotor modal damping. In this model,

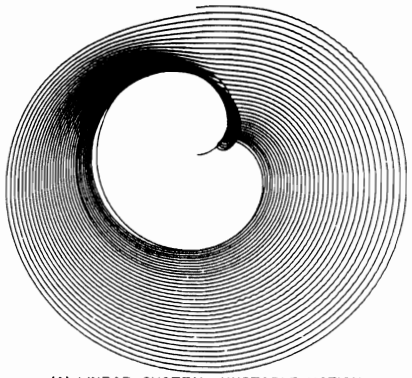

(A) LINEAR SYSTEM – UNSTABLE MOTION
NONSYNCHRONOUS PRECESSION
PREDOMINATES FOR N>20 CYCLES

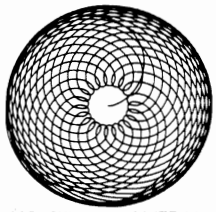

(B) NONLINEAR SYSTEM – FINITE LIMIT CYCLE
NONSYNCHRONOUS COMPONENT
REMAINS BOUNDED

Fig.7 Comparison of rotor half-frequency whirl motion at the threshold of stability - linear and nonlinear system

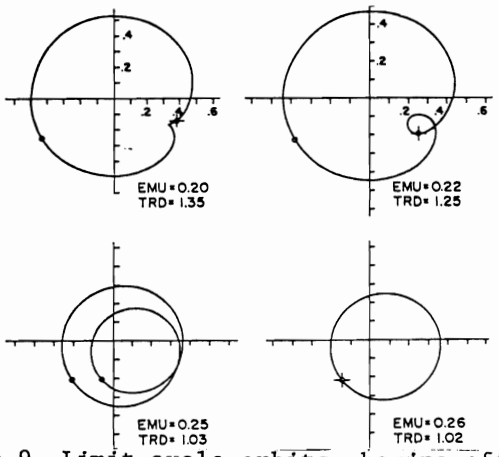


Fig.9 Limit cycle orbits showing effect of unbalance magnitude of motion of a journal - above stability threshold speed

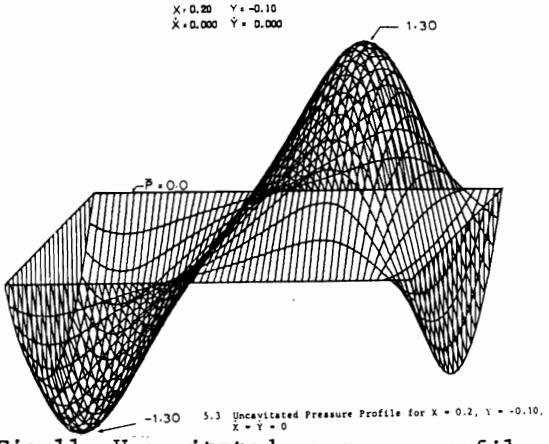


Fig.11 Uncavitated pressure profile

N = 10500 RPM
R = 1.00 IN.
L = 1.00 IN.
C = 5.00 MILS
TRSMAX = 20.89
S = 2.800
SS = 0.700
EMU = 0.80
SU = 0.224
TRDMAX = 1.67

WT = 1.00
W = 50 LB.
MUeS = 1.000 REYNS
FMAX = 1044.5 LB. AND
OCCURS AT 5.77 CYCLE
WS = 3.96
ES = 0.139
FU = 625.79 LB.
FURATIO = 12.52
ESU = 0.620

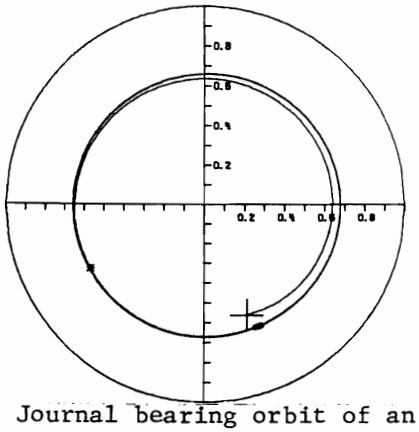

Fig.8 Journal bearing orbit of an unbalanced horizontal rotor above the stability threshold - synchronous limit cycle

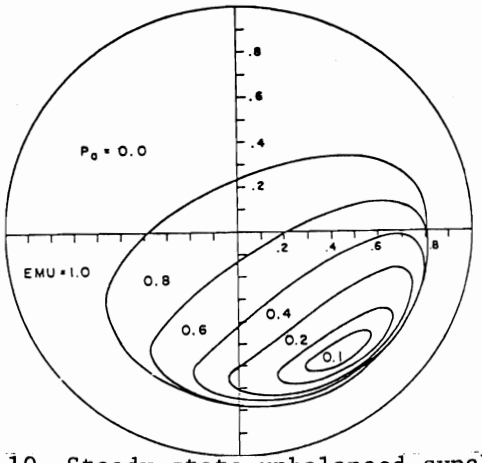


Fig.10 Steady state unbalanced synchronous whirl orbits for various values of dimensionless unbalance magnitude

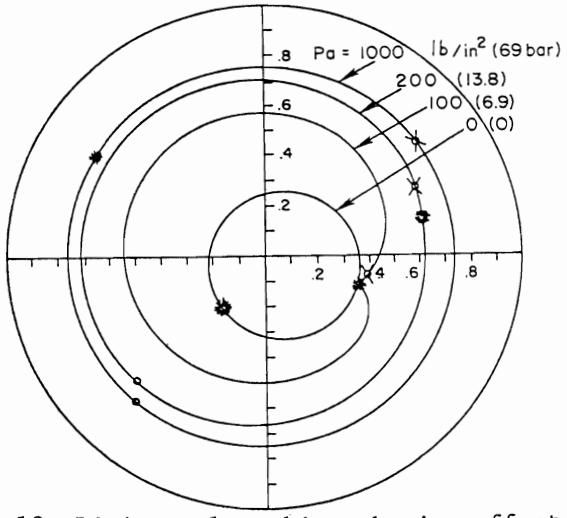


Fig.12 Limit cycle orbits showing effect of ambient pressure with optimum value of unbalance for 0 amb. press. N=10,500 RPM

the response is independent of the magnitude of the unbalance. Hence, the rotor amplitude of motion may be expressed in dimensionless form.

Rotor motion over a range of speeds assuming asymmetric linear bearing stiffness and damping characteristics is illustrated in Fig. 15. In this model, it is seen that the rotor forms elliptic orbits due to the asymmetric bearing stiffness and damping coefficients. This model, for example, has undamped critical speeds of $\omega_x$= 577 rad/sec and $\omega_y$=707 rad/sec due to the asymmetric bearing stiffness coefficients. Such behavior is commonly observed with tilting pad bearings. Upon approaching the stability threshold speed of 3,200 rad/sec, a large nonsynchronous whirl motion is encountered. For the linearized system, this whirl motion becomes unbounded. However, if nonlinear stiffening effects of the shaft are considered, a finite limit cycle results.

Fig. 16 represents the flexible rotor in linearized fluid film journal bearings with various amounts of nonlinear shaft stiffness considered. In the case of the linearized rotor-bearing system, the rotor is unstable at approximately twice the rotor undamped critical speed. The prediction of the rotor motion becoming unstable at approximately twice the rotor critical speed was first noted by Poritsky. For the linear system, the motion becomes unbounded once the stability threshold is reached. This is not necessarily the case with actual rotor-bearing systems. Depending upon the type of bearing used, various limit cycle orbits may be obtained. In Fig. 16, the parameter $\alpha$ represents the ratio of the shaft linear to the nonlinear cubic stiffness value included in the analysis. For a slight amount of nonlinear shaft stiffness, the shape of the critical speed curve changes. Also, it is observed that once the stability threshold is reached, a bounded limit cycle is obtained. This limit cycle increases with increasing speed. In actual systems, it has been observed that the limit cycle motion may remain constant over a large speed range and that at higher speeds under certain circumstances, the rotor system may even restabilize. Many of these characteristics can not be computed by ordinary linear stability theory.

Fig. 17 for example represents the various orbits obtained for different magnitudes of nonlinearity. For the linear system, it is noted that there is no limit cycle and that the motion increases with time. Orbits (b) and (c) represent finite limit cycles for the system. In all three cases, it may be stated that the rotor is operating above its stability threshold. However, in each case the actual magnitude of motion is dependent upon the nonlinear effects.

Fig. 18 represents the transient motion at the stability threshold for various values of the parameter $\alpha$. In Fig. 18A we see that the nonsynchronous component grows rapidly and becomes unbounded in the case of the linear system. In Fig. 18B for $\alpha$=0.01 a large but finite rotor orbit develops. As the value of $\alpha$ increases, the size of the limit cycle diminishes. For values of $\alpha$ exceeding 0.1, the nonsynchronous component is eventually suppressed, leaving only the synchronous precessive motion caused by rotor unbalance.

Experimental Rotor-Bearing Motion

Experimental data on a variety of vertical and horizontal test rotors with fluid film bearings has been obtained over the years in the Rotor Dynamics Laboratory of the University of Virginia. Fig. 19 shows a schematic diagram of the instrumentation setup. Experimental data may be collected and processed by an HP-9845B minicomputer using the Bently ADRE system, or data may be plotted directly from the digital vector filters to an analog plotter.

The actual motion of a flexible Bently rotor mounted in a plain journal bearing is shown in Fig. 20. For this particular test model, the rotor mass may be moved to vary the shaft flexibility effects. In this test, the mass was situated next to the bearing, simulating approximately a rigid rotor configuration. The rotor was run with 2 levels of unbalance. With the large level of unbalance, as shown in the lower figure, a nonlinear jump is observed at approximately 6300 RPM. Note that the synchronous motion is very similar to the analog computer prediction, as shown in Fig. 16 for $\alpha$=.1. The speed of 6300 RPM represents the nonlinear bearing critical speed. With the rotor unbalance reduced, as shown in the upper figure, the jump occurs at approximately the same speed of 6300 RPM. However, when the synchronous level reduces, a large nonsynchronous whirl motion occurs. It is therefore of interest to note that the overall vibration level above 6500 RPM is considerably higher for the balanced rotor.

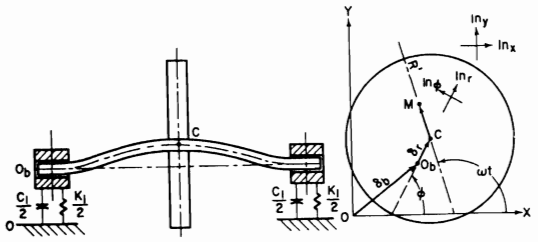


Fig.13 Flexible rotor bearing system

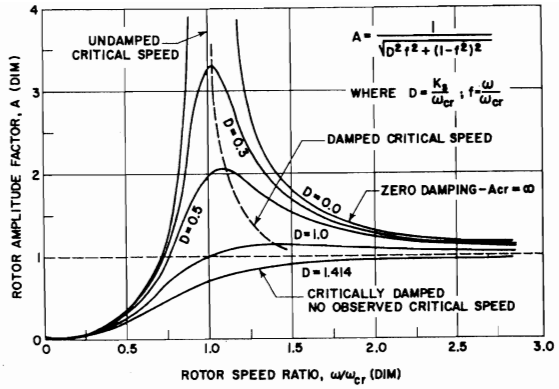


Fig.14 Rotor amplitude response for various damping values

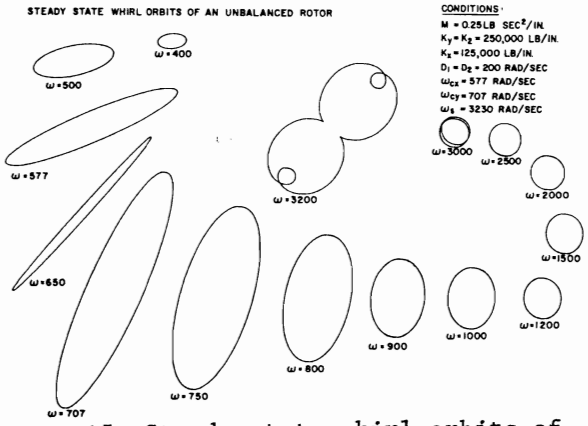


Fig.15 Steady state whirl orbits of an unbalanced rotor

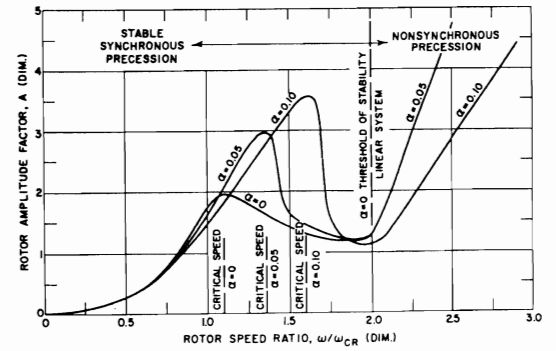


Fig.16 Nonlinear rotor motion for various α values

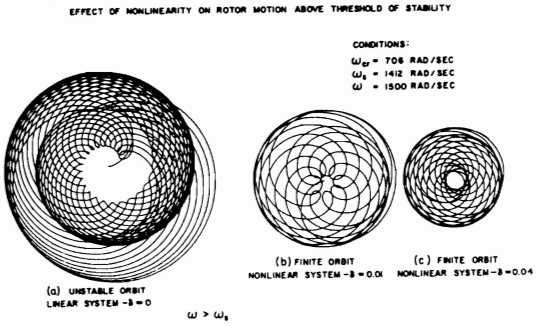


Fig.17 Effect of nonlinearity on rotor motion above the threshold of stability

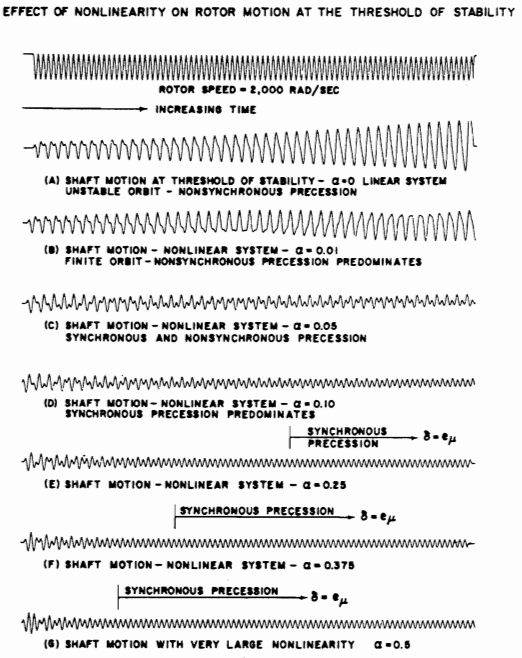


Fig.18 Effect of nonlinearity on rotor motion at the threshold of stability

Similar characteristic response curves are also observed in jet aircraft engines with oil squeeze film dampers. The oil squeeze film dampers have nonlinear characteristics similar to journal bearings under rotating loads. Fig. 21 shows the unbalance response of the gas generator of an aircraft engine for several unbalance levels. One can observe the abrupt nonlinear jump at the critical speed due to the squeeze film damper. Note that the jump speed may be shifted slightly depending upon the unbalance level in the rotor.

Fig. 22 represents a similar rotor system as shown in Fig. 20 except that the mass has been moved from the bearing location by 4.1 cm. A nonlinear jump is observed at 4700 RPM. The threshold of stability has been reduced due to the increased effects of shaft flexibility. The large nonsynchronous whirl motion appears to coincide with the nonlinear synchronous jump phenomena. When the synchronous motion jumps down, there is an abrupt increase in the nonsynchronous whirl motion. Note that from 5,000 to 10,000 RPM, the nonsynchronous limit cycle appears bounded. The system illustrated in Fig. 22 has a low unbalance level of 0.25 gm placed upon the rotor disk at a radius of 31.8 mm (1.25 in.). The vertical motion adjacent to the disk was monitored and the synchronous and total motion were simultaneously plotted on the analog plotter. When using the analog two pen plotter, a small pen offset is required. The stability onset speed corresponds closely to the predicted theoretical value which considers the linearized bearing and shaft stiffness effects.

The rotor system was operated under various levels of unbalance. Fig. 23 represents the rotor motion with the unbalance increased to 1.15 gm. With the increase in unbalance, it is seen that the stability threshold speed is reduced from 4700 RPM to 3600 RPM. There is a noticeable synchronous jump in the amplitude corresponding to the onset of instability. With the increased value of unbalance, an unusual phenomena is encountered at 5400 RPM at which the rotor system restabilizes. The motion between 5400 RPM and 7700 RPM is entirely synchronous precession. Between the operating speed of 5500 RPM and 8000 RPM, note that the amplitude of motion as shown in Fig. 23 is considerably smaller than the amplitude shown in Fig. 22 which has a low value of unbalance. Therefore, it is seen in this case that the introduction of moderate rotor unbalance has caused the system to restabilize above the initial onset speed of instability. At 8000 RPM, it is of interest to note that the rotor again becomes unstable. The self-excited whirl motion forms a limit cycle which increases with speed and becomes a maximum at approximately 9200 RPM. At speeds above this value, the limit cycle remains constant.

Foundation effects can also play an important role in the dynamic response and stability characteristics of rotors in fluid film bearings. In Fig. 24, the rotor system was placed upon a foam isolation pad. Some noticeable effects in the stability characteristics were observed. With the rotor on the isolation pad, with the unbalance of 1.15 gm, the rotor stability threshold increased from 3700 RPM to 4100 RPM. The rotor again exhibited the restabilization characteristic at a higher speed of 6300 RPM. However, it showed the unusual effect that with the rotor on the foam foundation, no instabilities were encountered at higher operating speeds. The rotor now was completely stable above 6300 RPM. The self-excited whirl phenomena in this case was limited to an operating speed of 4000 to 6300 RPM.

Fig. 25 represents the single mass flexible rotor mounted in the plain journal bearing with the mass located at the quarter span and well balanced. By moving the mass further away from the fluid film journal bearing, the stability threshold of the system has been reduced even further to 2000 RPM. Fig. 25 shows the trace of the synchronous and total motion. The total motion forms a relatively constant limit cycle over the entire operating speed range of 2000 to 7000 RPM. From the observation of the trace of the synchronous motion there appears to be a flexible rotor critical speed at 5000 RPM. The presence of a system critical speed is also indicated by the phase angle change as seen in the upper trace.

Although the rotor is in whirl from 2000 RPM and higher, the characteristics of the whirl motion changes dramatically at 8000 RPM. Fig. 26 represents the frequency spectrum vs speed for the flexible rotor mounted at the shaft quarter span. For the speed range of 2000 to 8000 RPM, the whirl motion is approximately half frequency whirl. Above 8000 RPM, there can be seen a distinct change in

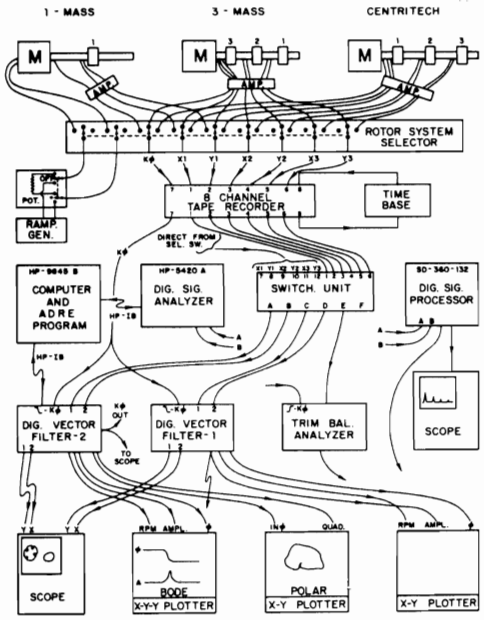


Fig.19 Instrumentation block diagram

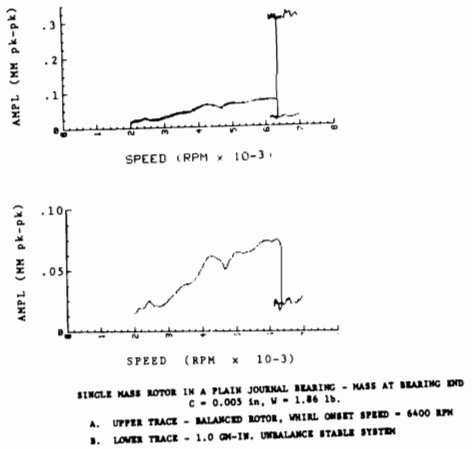


Fig.20 Single mass rotor in a plain journal bearing-mass at bearing end

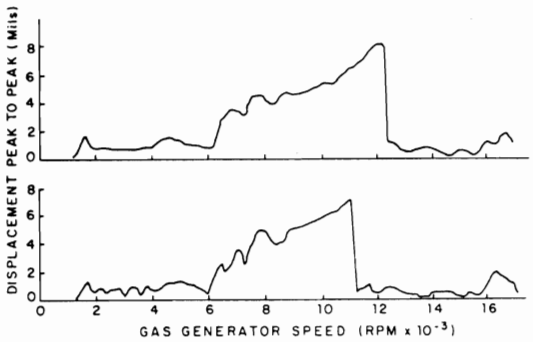


Fig.21 Gas generator nonlinear response

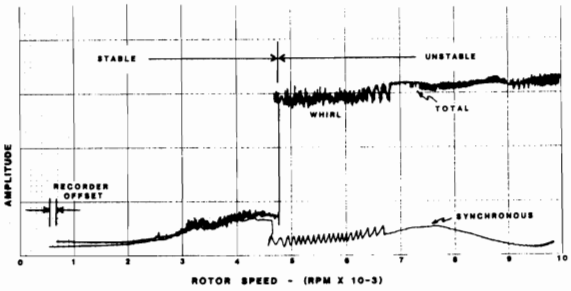


Fig.22 Single mass flexible rotor in a plain journal bearing-mass 4.1 cm from bearing end--unbalance = 0.25 gm

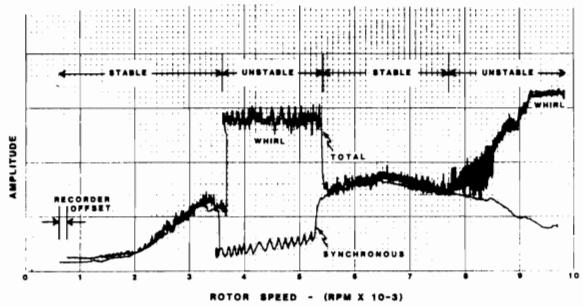


Fig.23 Single mass flexible rotor in a plain journal bearing-mass 4.1 cm from bearing end--unbalance = 1.15 gm

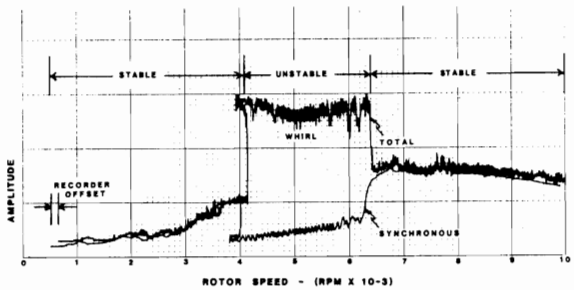


Fig.24 Single mass flexible rotor in a plain journal bearing-mass 4.1 cm from bearing end--unbalance=1.15 gm--system on isolation pad

the frequency spectrum. The nonsynchronous motion is no longer at one-half frequency, but is now tracking approximately the shaft resonant frequency of 4000 RPM. This phenomena is known as resonant whip. Therefore, above 8000 RPM the rotor motion changes from half frequency oil whirl to resonant shaft whip which excites the rotor system first natural flexible critical speed. For this case of low unbalance, the system remains highly unstable throughout the entire operating speed range.

When a large amount of rotor unbalance of 1.5 gm is added, the rotor stability characteristics change considerably as seen in Fig. 27. The onset of self-excited whirl has not been dramatically shifted and is observed to occur at approximately 2300 RPM. A constant limit cycle of motion is obtained from 2300 to 4000 RPM. At 4000 RPM when the synchronous amplitude of motion increases due to the system resonant frequency, the rotor motion is stabilized. At this point, the self-excited whirl motion is suppressed. Upon passing through the rotor critical speed, the rotor remains in stable synchronous precession. The rotor however may jump unstable at higher operating speeds. The interesting paradox has been found with this system that it is possible to operate above the stability threshold with lower levels of vibration by having large values of unbalance in the rotor. It has been observed that balanced rotors operating above the stability threshold with both rigid and flexible shafts in plain journal bearings often had higher limit cycles of motion than did the rotor systems with moderate to large unbalance levels.

Fig. 28 represents a schematic diagram of a vertical test rig used to test various rotor mass and bearing combinations. Fig. 29 for example shows the response of a three-mass configuration in which the rotor has two critical speeds. These critical speeds are 1650 RPM and 6325 RPM. The bearings used in this case are porous bronze bearings with marginal lubrication. The upper trace represents the synchronous phase angle and the lower plot represents the synchronous and total shaft motion. It is seen that after the rotor passes through its second critical speed, the rotor becomes unstable at 6700 RPM. The nonsynchronous motion in this case increases with speed. A further increase in speed above 10,000 RPM could cause the noncontacting proximity probes to wipe or could cause bearing damage. Another model was tested in which the bearing span was increased to cause 3 critical speeds to be in the operating speed range.

Fig. 30 represents the undamped critical speed mode shapes corresponding to the experimental data as shown in Fig. 29. It is apparent, from the observation of the second critical speed mode shape of Fig. 30, that high bearing forces and displacements are encountered at the second critical speed of 6325 RPM. As the system passes through the second critical speed, there is a reduction in the bearing loading, At 6700 RPM, the rotor becomes unstable and rotor resonance whip is encountered in which the first rotor critical speed is excited.

To investigate the possibility that the bearing loading caused by operation near a critical speed could effect stability, a rotor system was tested with a longer bearing span of 610 mm (24 in.). This system is similar to the rotor system shown in Figs. 29 and 30, except that the extended bearing span causes three flexible critical speed modes to be in the operating speed range. The animated rotor first three critical speeds are shown in Figs. 31-33. The rotor mode shapes shown are for the single-dual bearing configuration in which two bronze bushing bearings were used to control stability. Significant factors concerning the influence of rotor unbalance on bearing induced stability, is whether the rotor is operating in the vicinity of a critical speed; and also the relative strain energy distribution between the elastic rotor and bearings.

A cascade spectrum of the three-mass vertical rotor with the single bearing configuration is shown in Fig. 34. The plot represents the rotor operating speed vs the frequency spectrum. The frequency spectrum on the 45° axis represents the rotor response due to unbalance. In this rotor system, it is seen that at 3300 RPM the rotor becomes unstable and subsynchronous precession develops, corresponding to the rotor first critical speed. As the operating speed increases, the subsynchronous whirl frequency increases slightly due to the gyroscopics of the rotor system. At 9000 RPM, there is a strong subsynchronous component of motion. After operation over an extended period of time at this elevated speed, the rotor became substantially bowed affecting the first mode unbalance. Upon rerunning, a large first critical response was obtained. Large amounts of unbalance in the first mode had little effect on the rotor instability threshold.

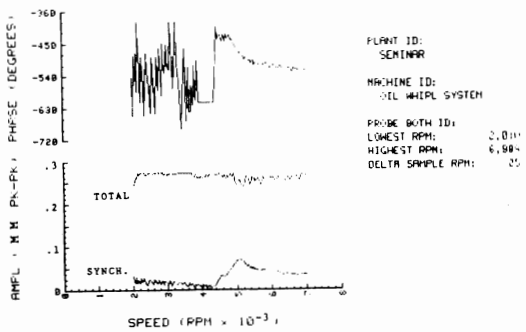


Fig.25 Single mass flexible rotor in a plain journal bearing--mass at quarter span

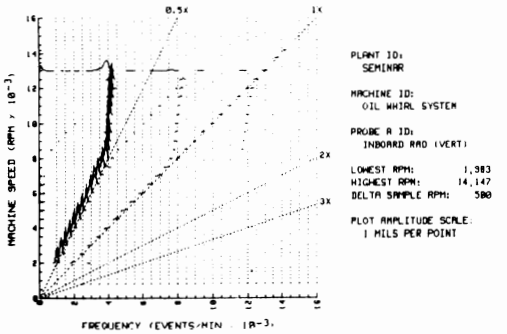


Fig.26 Frequency spectrum vs speed of a single mass flexible rotor in a plain journal bearing-mass at quarter span

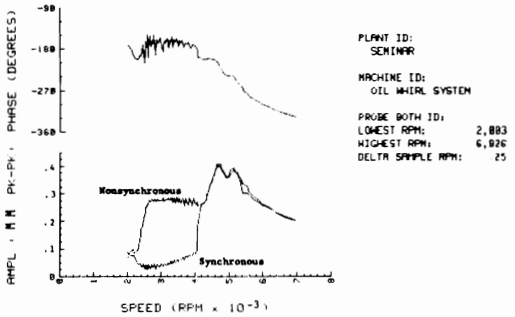


Fig.27 Single mass flexible rotor in a plain journal bearing with large unbalance--mass at quarter span

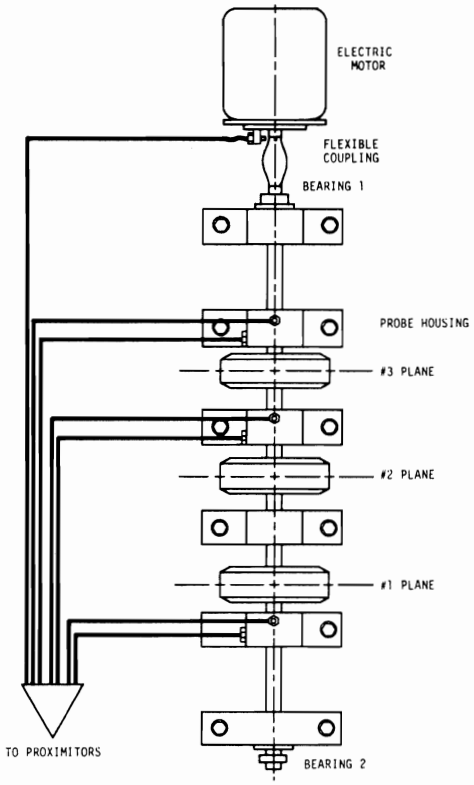


Fig.28 Vertical three-mass flexible rotor

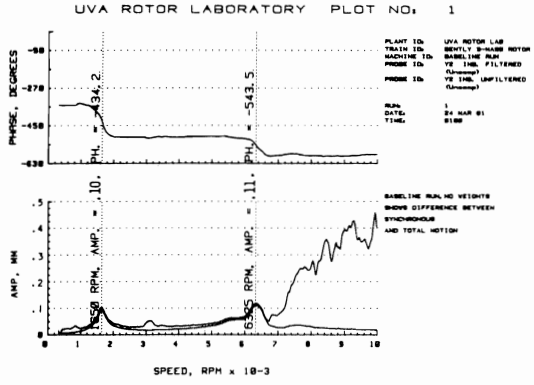


Fig.29 Bode plot of vertical three-mass flexible rotor--16" bearing span

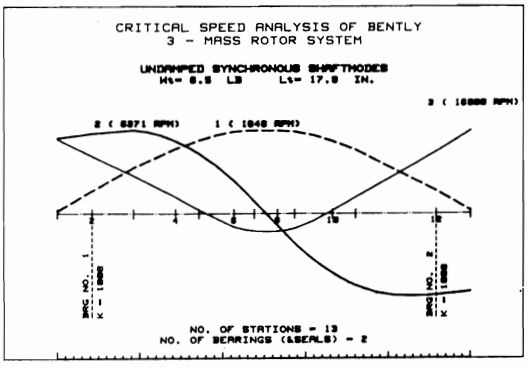


Fig.30 Undamped synchronous mode shapes of three-mass rotor with 16" bearing span

A possible reason for this is that over 90% of the strain energy in the system is associated with the flexible shaft for the first mode. Hence, bearing loading is low.

Fig. 35 represents the synchronous and direct motion taken at the horizontal center span of the three-mass rotor mounted on single bearings. It can be seen that at a speed as low as 2300 RPM, the rotor becomes unstable as shown by the deviation of the nonsynchronous from the synchronous motion. When the rotor begins to enter the second critical speed at 2700 RPM, the rotor is stabilized due to the application of large forces transmitted to the bearings. Upon passing through the second critical speed, the rotor becomes unstable again at 3000 RPM. As the rotor speed is increased, the nonsynchronous component also increases in magnitude and reaches a maximum value of approximately 0.7 mm (28 mils) at 6500 RPM. At this speed, the nonsynchronous amplitude collapses due to the approach of the third critical speed. The nonsynchronous motion is suppressed while the rotor is passing through the third critical speed. It can be seen from this figure that as long as the synchronous amplitude of motion is above 0.13 mm (5 mils) at the rotor center, the nonsynchronous whirl motion is suppressed. As the rotor passes through the third critical speed and the synchronous amplitude diminishes below 0.13 mm (5 mils) at a speed of 8500 RPM, the nonsynchronous motion again rapidly builds up.

A cascade spectrum is shown in Fig. 36 of the three-mass vertical rotor in which a dual bronze bushing bearing was added at the lower rotor end in order to control the self-excited instability. The animated critical speeds as shown in Figs. 31-33 correspond to this system. In Fig. 36, it is noted that there is no self-excited whirl motion present until a speed of 8000 RPM is reached. At this speed, the first critical speed is excited. Upon entering the third critical speed, the subsynchronous whirl motion is suppressed. From the observation of the spectrum along the 45° line, it is seen that a considerable amount of rotor unbalance is present in all three modes. After the rotor was carefully balanced for the first and second modes, the stability threshold was considerably reduced.

In the process of balancing the rotor through its various modes, it was found that the level of modal unbalance distribution could have a profound effect on the occurrence of self-excited whirl instability. In general when self-excited whirl motion occurred, the frequency of excitation normally corresponded to the first mode. However, under certain conditions, an excitation of the second mode would briefly occur as shown in Fig. 36 at a speed of 7250 RPM.

Fig. 37 represents the rotor synchronous and direct motion for well balanced first and second critical speeds. The high total motion observed at 500 RPM indicates that the rotor system is very sensitive to external excitation and self-excited whirl mechanisms. There is a strong nonsynchronous excitation when the rotor is operating at one-half its first critical speed. A two times excitation in the system can be generated by coupling misalignment. However, if the secondary harmonic or "secondary critical" is large, then this indicates an extremely sensitive system. If this phenomena is observed in an actual turborotor, then one should not operate it to higher speeds. A bearing or shaft redesign is indicated.

As the rotor balancing is improved, the stability threshold speed reduces to approximately twice the rotor first critical speed and the system is unstable at all higher speeds. This is a case of classic resonant whip. For the various vertical rotors tested in the bronze bushing bearings, it was found that the total motion running near the second or third critical speed with large unbalance may be paradoxically smaller than is the case for the total motion with a well balanced rotor. It is apparent and well known that one should not operate, for example, a vertical flexible rotor in plain cylindrical bearings because of the inherent stability problems. For those manufacturers who insist upon violating this fundamental principle, one should exercise care in not achieving too high a level of rotor balance.

In the field of turbomachinery, the speed of turbocompressors has shown a dramatic increase from the late 1950's to the present day designs. In the 1950's, machine speeds were generally limited to below 7000 RPM. However, today, multistage compressors are running at 12,000 to 14,000 RPM in tilting pad bearings. A significant number of stability problems have been encountered with this class of compressor. The Centritech research rig was developed for the

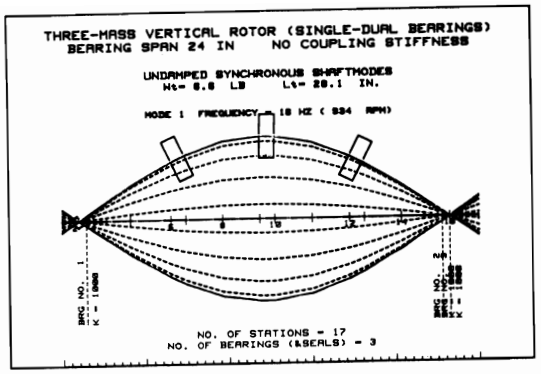


Fig.31 Animated mode shape plot for the first critical speed three-mass vertical rotor--24" bearing span

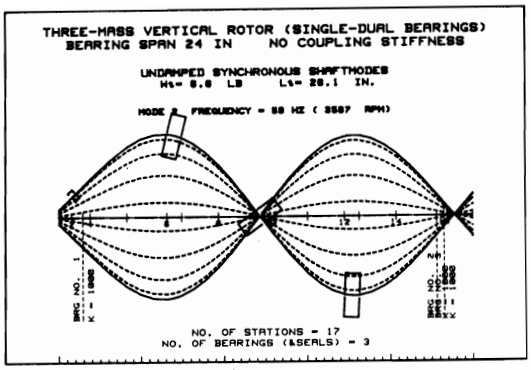


Fig.32 Animated mode shape plot for the second critical speed three-mass vertical rotor--24" bearing span

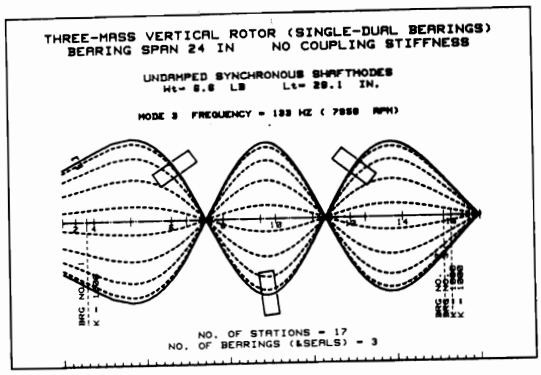


Fig.33 Animated mode shape plot for the third critical speed three-mass vertical rotor--24" bearing span

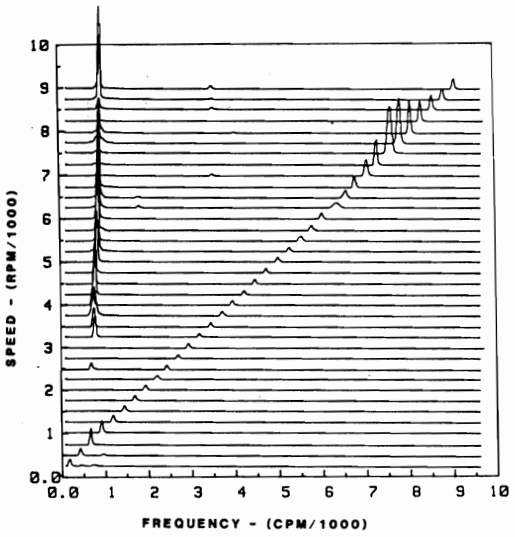


Fig.34 Cascade spectrum of three-mass vertical rotor--24" bearing span--single bearing system

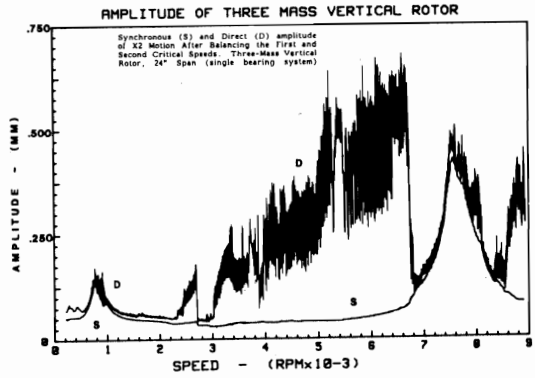


Fig.35 Three-mass vertical rotor, Y2 motion after balancing the first and second critical speeds--24" bearing span--single bearing system

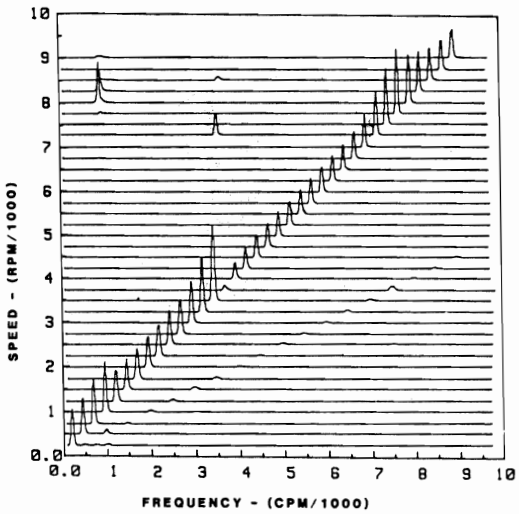


Fig.36 Cascade spectrum of three-mass vertical rotor--single-dual bearing system--24" bearing span

University of Virginia Rotor Dynamics Laboratory (see Fig. 38) to simulate an 8-stage compressor operating at 12,000 RPM with its first critical speed between 2500 to 4000 RPM. One of the objectives of the research program was to evaluate various bearing configurations on this test rig to determine which bearings had the highest stability characteristics and could be used for machines operating above 12,000 RPM.

Fig. 39 for example represents the stability characteristics of three lobe bearings with various preloads. For the case of the rigid rotor, the stability of a preloaded three lobe bearing increases rapidly for Summerfeld numbers exceeding 5. This represents a lightly loaded bearing. No such effect is obtained with the plain journal bearing. These various stability plots are based on linearized fluid film bearing theory.

Fig. 40 shows the bearing-motion of a flexible rotor in plain journal bearings with a radial clearance of 25.4 μm (.001 in.). The upper trace represents the total motion for acceleration and deceleration and the bottom trace represents the synchronous motion. At a speed of approximately twice the rotor first critical speed of 2850 RPM, the instability onset speed occurs. This speed is 5750 RPM. As the rotor speed is increased above the onset speed, a limit cycle is observed at the bearing probe. Upon coast down, a torsional lateral coupling excitation was observed. When the rotor speed was reduced, a resonant whip was encountered at 5350 RPM. This phenomena was never encountered upon acceleration. It is also of interest to note that the amplitude of motion for acceleration and deceleration are different. If acceleration is included in the equations of motion, the system is nonlinear. From a balancing standpoint, it is important to consistently take the readings either with speed increasing or reducing, but not to mix the measurments because of the shifting of the amplitude and phase response due to the acceleration effects.

Another important nonlinear effect to observe, in Fig. 40, is the secondary critical speed response at 1375 RPM. This secondary critical speed excitation was observed only upon acceleration and never upon deceleration. It is believed caused by the effect of the coupling on the rotor response. For this rotor system, the application of large levels of unbalance of the rotor had little effect on changing the stability threshold and the limit cycle motion above 6000 RPM. This is believed due to the high flexibility of the rotor system and the high ratio of the shaft strain energy to the bearing energy.

In most turbocompressors, the amplitude of motion is observed near the bearings. When the amplitude of motion is observed at the rotor center, substantially larger amplitudes of motion are seen. The peak amplitudes of motion observed at the center as compared to the bearing locations do not necessarily correspond to the same speed. Fig. 41 represents the horizontal center span motion with plain journal bearings. Upon acceleration, there is a substantially lower critical speed response obtained than for the case of slow deceleration. Note also that the acceleration-deceleration rate can shift the occurrence of the critical speed. Upon reaching 5900 RPM, the rotor goes into a large limit cycle whirl of approximately 0.11 mm (4.5 mils). When the speed is reduced, the rotor encounters a large resonant whip at 5500 RPM of over 0.14 mm (5.5 mils). This large resonant whip motion occurring on deceleration could be dangerous in an actual turborotor, causing bearings and seals to whip. It is readily apparent that it would be undesirable to employ a plain journal bearing in a turbocompressor operating at 12,000 RPM with a critical speed of 3000 to 4000 RPM. The first mode unbalance has little effect in stabilizing the rotor.

The plain journal bearing has very poor stability characteristics. In order to improve the stability characteristics of plain bearings, various design changes have been used in the past such as grooves, multiple lobes or pressure dams. The object of a pressure dam bearing, for example, is to generate a loading on the top of the shaft by means of a step.

Fig. 42 shows the synchronous and direct motion with a well balanced rotor using pressure dam bearings with an excessive dam depth. For the case of a pressure dam bearing with excessive recess clearance, no improvement in stability is achieved, compared to the plain journal bearing. The rotor becomes violently unstable at 5600 RPM and does not possess a limit cycle which gradually increases in speed, but rather abruptly jumps in a large limit cycle whirl motion. Operation above the stability threshold of a turbocompressor with a

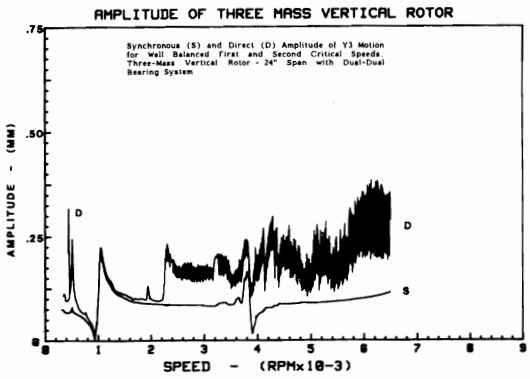


Fig.37 Three-mass vertical rotor, Y3 motion for well-balanced first and second critical speeds--24" bearing span--dual dual bearing system

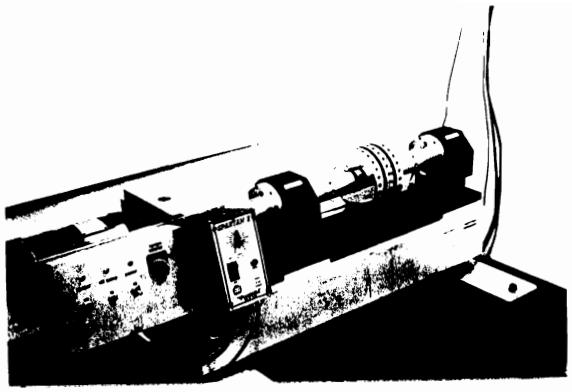

Fig.38 Centritech Test Rotor No. 1

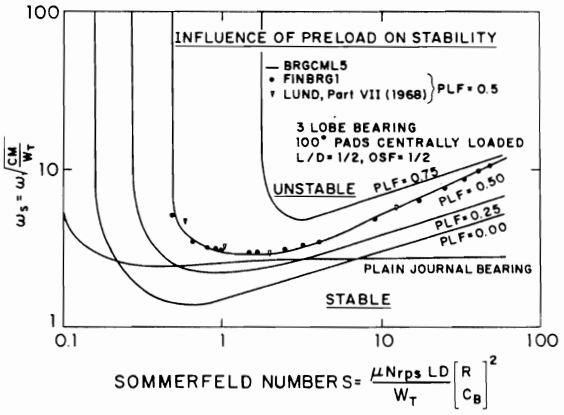


Fig.39 Influence of preload on stability for various three-lobe bearings

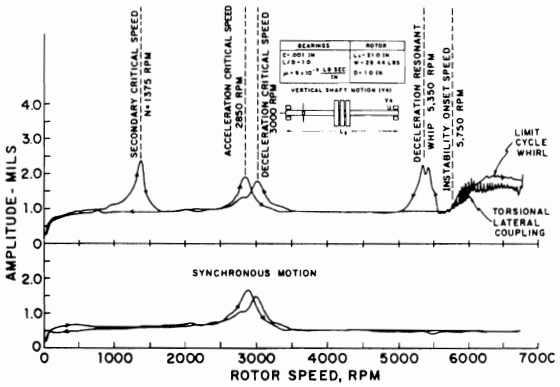


Fig.40 Centritech Test Rotor No. 1--plain journal bearings

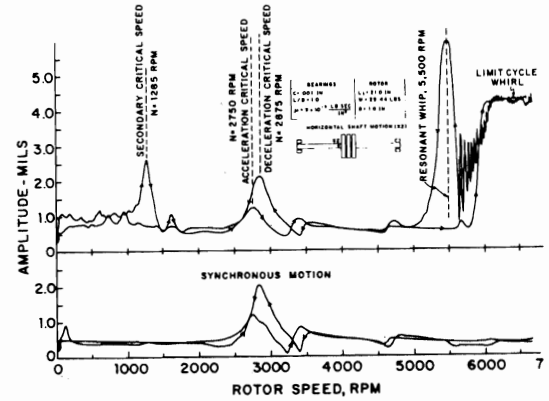


Fig.41 Centritech Test Rotor No. 1--plain journal bearings--center shaft motion

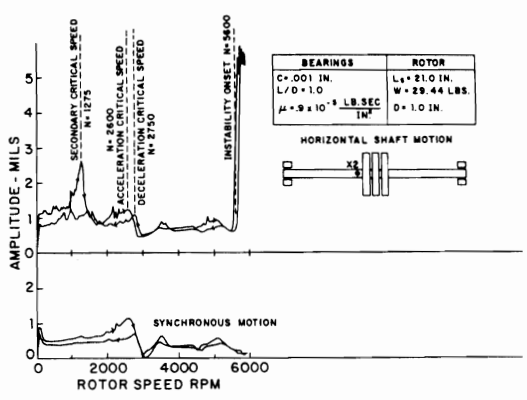


Fig.42 Centritech Test Rotor No. 1-test compressor-pressure dam bearings-nonoptimum design-center shaft motion

pressure dam bearing could be catastrophic. Unbalance in the first mode has relatively little effect in changing either the onset speed or the nature of the limit cycle with the pressure dam bearing.

Fig. 43 represents the motion of the Centritech test rotor with optimal design pressure dam bearings. The dam height to clearance ratio was reduced from over 10 to 2.8. By reducing the dam height, it is seen that the stability threshold is dramatically improved from under 6000 to over 9500 RPM (Leader). However, a similar whirl behavior was encountered with the optimal design pressure dam bearing as was observed with the previous case. That is, upon the onset of whirl instability, the limit cycle of motion became extremely large and almost unbounded. Rotor unbalance had little effect on the size of the nonsynchronous limit cycle. Experimental testing therefore indicates that it is dangerous to exceed the stability threshold of a pressure dam bearing because of its inability to have well bounded limit cycle motion. This type of large nonsynchronous motion has resulted in the destruction of turbines exceeding the stability threshold when operating with pressure dam bearings. Another bearing type tested by Leader was the four lobe bearing with a preload of 0.77. A stability threshold of 9500 RPM was obtained with this system as shown in Fig. 44. Upon shutdown, an amplitude of over 0.76 mm (30 mils) was obtained at the rotor center. A considerable hysteresis region was encountered upon speed reduction. The rotor did not completely restabilize until an operating speed of 7300 RPM was obtained. This characteristic of a hysteresis region is very common in plain or fixed lobed hydrodynamic journal bearings. That is, once the system becomes unstable, there is a low speed which the rotor must attain to restabilize. When the rotor goes into a large amplitude whirl motion, the bearing characteristics are no longer represented by linearized coefficients. This nonlinear effect in the bearing leads to the hysteresis region. No hysteresis region was encountered with the pressure dam bearing. This may be due to the effect of the pressure dam on the hydrodynamic film with large orbiting.

One of the most stable bearing types is the offset-half bearing. The offset-half bearing was tested with a radial clearance of 51 μm (.002 mils). When the rotor was balanced, the onset of instability occurred at approximately 6900 RPM as shown in Fig. 45. A controlled limit cycle motion was obtained. At 8000 RPM, a total peak to peak motion was approximately 0.20 mm (8 mils). The critical speed for this system was about 2700 RPM. Rotor unbalance in the first mode had relatively little effect on the onset of instability with the 51 μm (2 mils) clearance bearing. However, when unbalance was placed to excite a second mode of response, the motion was completely synchronous. As can be seen from Fig. 46, the synchronous motion continued to increase from 3000 to 8000 RPM with no indication of self-excited whirl motion. The second mode unbalance placed upon the rotor generates large rotating forces which stabilizes the system. However, with the large unbalance in the rotor, the system could not be safely operated above 8000 RPM due to the excessive bearing forces transmitted and the large synchronous amplitudes.

Fig. 47 represents a system similar to Fig. 46, except that an extremely tight offset-half bearing was tested with a radial clearance of 13 μm (.5 mils). Several unusual nonlinear effects were present in this system due to the bearing clearance. The theoretical rigid bearing critical speed for this test system is approximately 2600 RPM. However, it is seen from the experimental data that a critical speed of 3074 RPM is obtained. This increase in the rotor critical speed is due to the effective shaft span reduction due to the shaft contacting the bearing shoulders. This, in effect, creates a nonlinear shaft stiffness. The shape of the critical speed response appears truncated due to the close fitting bearings. At approximately twice the rotor critical speed, 7000 RPM, a violent instability occurs and then the rotor restabilizes at 7400 RPM. Above 7500 RPM the rotor is completely stable. However, the large nonsynchronous whirl motion encountered at about 7000 RPM has led to probe wiping and bearing metal-to-metal contact with the shaft. Although the close clearance offset-half bearing has the highest stability characteristics of the family of multilobe bearings, it is apparent that it would be an undesirable candidate for application in a high speed turbocompressor designed to operate in the 12,000 to 14,000 RPM range.

Fig. 48 represents the synchronous and total motion with a five-pad tilting

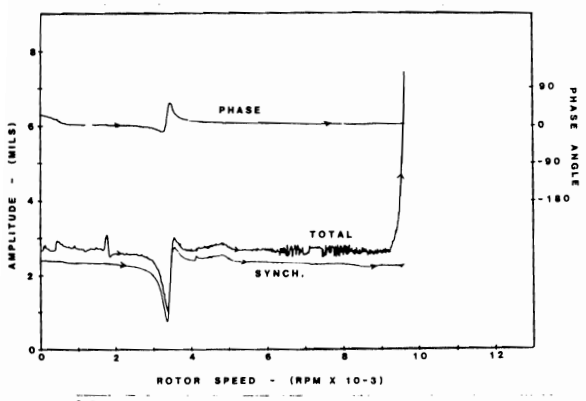


Fig.43 Centritech Test Rotor No. 1--optimized pressure dam bearings--center shaft motion

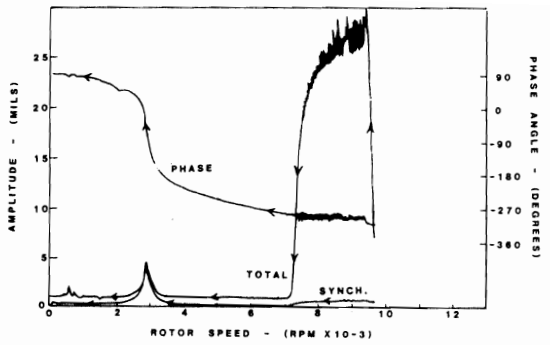


Fig.44 Centritech Test Rotor No. 1-four-lobe bearings, preload=0.77

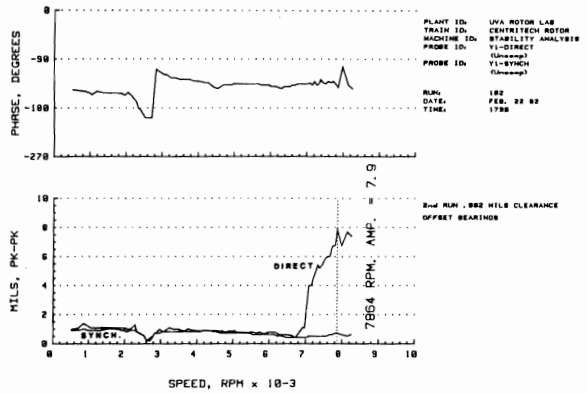


Fig.45 Centritech Test Rotor No. 1--offset--half bearings--0.002 mils clearance

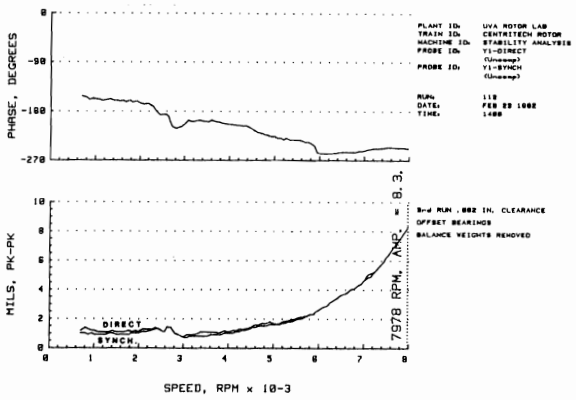


Fig.46 Centritech Test Rotor No. 1--offset--half bearings--0.002 mils clearance, balance weights removed

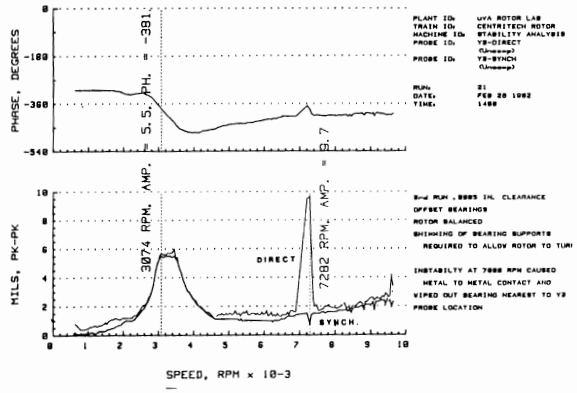


Fig.47 Centritech Test Rotor No. 1--offset--half bearings--0.0005 mils clearance, balance weights removed

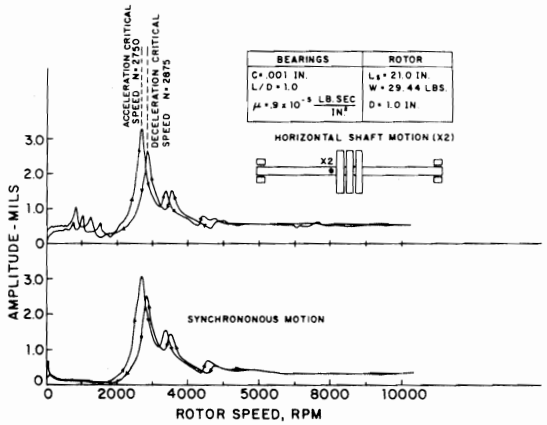


Fig.48 Centritech Test Rotor No. 1--tilting five-pad bearings

pad bearing. This bearing type has seen a considerable usage in high speed turborotors. From the observation of the synchronous and total motion, it is noted that there is no nonsynchronous motion present in the operating system up to 10,500 RPM. Upon carefully balancing the rotor, no whirl motion was observed. Balancing has no effect on self-excited whirl motion. The unbalance response characteristics with the tilting pad bearings are reasonably linear for a range of 40% of the bearing clearance. When self-excited whirling occurs in practice with centrifugal compressors with tilting pad bearings, the excitation forces are normally not associated with the bearings, but are caused by other effects such as aerodynamic cross-coupling or seals. Under these circumstances, the level of rotor unbalance does not have a substantial effect on changing the stability characteristics of the system.

## CONCLUSIONS

1. Nonlinear effects are present in various degrees in all turborotors. Nonlinear effects may have an important influence on the character and nature of rotor synchronous and nonsynchronous response.
2. Nonlinear rotor-bearing characteristics may be caused by fluid film bearings and seals, shafts, couplings, bearing deadbands, misalignment and rotor acceleration rates.
3. Nonlinear effects are responsible for super and subharmonic oscillations, jump phenomena and for the occurrence of limit cycle motion when operating above the rotor stability threshold.
4. The rotor-bearing nonlinearities in combination with unbalance may cause jump phenomena to occur at the critical speed.
5. The onset speed of instability may be altered due to the level of rotor unbalance with fluid film bearings.
6. Nonlinear effects are important in limiting the severity of motion when self-excited whirl is encountered.
7. A synchronous jump down (or up) in rotor amplitude is often associated with the onset of instability (or restabilization) with fluid film bearings.
8. Rotor restabilization and whirl suppression by the application of unbalance may occur with fluid film bearings operating above the stability threshold.
9. The jump speed (or speed of restabilization) cannot be predicted by linearized rotor-bearing theory.
10. Time-transient computer simulations are time consuming and expensive, but are useful in the simulations of nonlinear effects generated by bearings, seals, squeeze film dampers, etc.
11. Multiplane balancing programs are based upon linearized rotor-bearing theory. In practice, several iterations of balance may be necessary due to various nonlinear effects.
12. Rotors with moderate levels of unbalance in fluid film bearing systems may actually have lower levels of total motion than a well balanced rotor.
13. Various fluid film bearings exhibit different limit cycle behavior above the stability threshold. A rotor may be operated well above its stability threshold if it has a well bounded limit cycle.
14. For flexible rotor-bearing systems in which the shaft whirl motion has over 90% of the system strain energy, first mode unbalance has little effect in altering the system limit cycle motion.
15. A pressure dam bearing supported rotor is dangerous to operate above its stability threshold due to the apparent unbounded nature of the whirl motion.
16. When balancing a rotor, nonsynchronous as well as synchronous motion should be monitored. A well balanced rotor may result in bearing damage.
17. With a vertical flexible rotor in plain or lobed bearings, it may be desirable to have the rotor operating at or near a second or third critical speed.
18. The tilting pad bearing is relatively free from self-excited fluid film whirl and rotor unbalance will not excite or induce whirl motion.
19. Whirl motion observed in tilting pad turborotors operating at multiples of the first critical speed is often associated with aerodynamic or seal effects; rotor stabilization cannot usually be achieved by changing rotor balance level.

REFERENCES


1. Adams, M. L., "Nonlinear Dynamics of Flexible Multi-Bearing Rotors," Journal of Sound and Vibration, Vol. 71, No. 1, 1980, pp. 129-144.

2. Adams, M. L., Padovan, J., and Fertis, D. G., "Engine Dynamic Analysis with General Nonlinear Finite-Element Codes, Part I: Overall Approach and Development of Bearing Damper Element," ASME Paper 81-GT-151, Gas Turbine Conference, March 1981.

3. Allaire, P. E., Barrett, L. E., and Gunter, E. J., "Variational Method for Finite Length Squeeze Film Dampers with Applications," Wear, Vol. 42, Jan. 1977, pp. 9-22.

4. Allaire, P. E., Nicholas, J. C., and Gunter, E. J., "Systems on Finite Elements for Finite Bearings," Journal of Lubrication Technology, TRANS. ASME, Vol. 99, Series F, No. 2, Apr. 1977, pp. 187-197.

5. Barrett, L. E., and Gunter, E. J., "Steady-State and Transient Analysis of a Squeeze Film Damper Bearing for Rotor Stability," NASA Contract Report, Federal Scientific and Technical Information, Springfield, Virginia, NASA CR-2548, May 1975.

6. Barrett, L. E., Gunter, E. J., and Allaire, P. E., "Stability and Dynamic Response of Pressurized Journal Bearings with Nuclear Water Pump Applications," Annals of Nuclear Energy, 1977.

7. Barrett, L. E., Gunter, E. J., and Akers, A., "Effect of Unbalance on a Journal Bearing Undergoing Oil Whirl," Institute of Mechanical Engineering, Tribiology Group, Proceedings, Vol. 190, 1976, pp. 31-76.

8. Barrett, L. E., Allaire, P. E., and Gunter, E. J., "The Dynamic Analysis of Journal Bearings Using a Finite Length Correction for Short Bearing Theory," ASME Proceedings, Topics in Fluid Film Bearing Design and Optimization, Apr. 1978, pp. 29-42.

9. Barrett, L. E., and Gunter, E. J., "Stabilization of Aerodynamically Excited Turbomachinery with Hydrodynamic Journal Bearings and Supports," NASA Conference Publication 2133, Symposium on Rotordynamic Instability Problems in High Performance Turbomachinery, 1980.

10. Bently, D. E., "Forced Subrotative Speed Dynamic Action of Rotating Machinery," ASME Paper 74-PET-16, Petroleum Mechanical Engineering Conference, Sept. 1979.

11. Childs, D. W., "Fractional-Frequency Rotor Motion Due to Nonsymmetric Clearance Effects, " ASME Paper 81-GT-156, Mar. 1981.

12. Choy, K. C., Gunter, E. J., and Allaire, P. E., "Fast Fourier Transform Analysis of Rotor-Bearing Systems," ASME Proceedings, Topics in Fluid Film Bearing Design and Optimization, Apr. 1978, pp. 245-272.

13. Christensen, E., Tonnesen, J., and Lund, J. W., "Dynamic Film Pressure Measurements in Journal Bearings for Use in Rotor Balancing," Journal of Engineering for Industry, TRANS. ASME, Series B, Vol. 98, No. 1, Feb. 1976, pp. 92-100.

14. Cunningham, R. E., Fleming, D. P., and Gunter, E. J., "Design of a Squeeze Film Damper for a Multi-Mass Flexible Rotor," Journal of Engineering for Industry, TRANS. ASME, Vol. 97, Series B, No. 4, Nov. 1975, pp. 1383-1389.

15. Ehrich, F. F., "Subharmonic Vibrations of Rotors in Bearing Clearance," ASME Paper 66-MD-1, Design Engineering Conference, May 1966.

16. Falkenhagen, G. L., Gunter, E. J., and Schuller, F. T., "Stability and Transient Motion of a Vertical Three-Lobe Bearing System," Journal of Engineering for Industry, TRANS. ASME, Vol. 94, Series B, No. 2, May 1972, pp. 655-677.

17. Falkenhagen, G. L., and Gunter, E. J., "Nonlinear Transient Analysis of a Rigid Rotor Supported by Non-Circular Bearings," Report No. ME-4040-102-70U, June 1970, 191 p., University of Virginia.

18. Flack, R. D., Leader, M. E., and Gunter, E. J., "An Experimental Investigation on the Response of a Flexible Rotor Mounted in Pressure Dam Bearings," Journal of Engineering for Power, TRANS. ASME, Vol. 102, Oct. 1980, pp. 842-850.

19. Gunter, E. J., "Dynamic Stability of Rotor-Bearing Systems," NASA SP-113, Office of Technical Utilization, U.S. Government Printing Office, Washington, D.C., 1966, 288 p.

20. Gunter, E. J., "Rotor-Bearing Stability," Proceedings of First Turbomachinery Symposium, Texas A & M University Press, Oct. 1972, pp. 119-141.

21. Gunter, E. J., Barrett, L. E., and Allaire, P. E., "Design and Application of Squeeze Film Dampers for Turbomachinery Stabilization," Proceedings of the Fourth Turbomachinery Symposium, Texas A & M University Press, Oct. 1975, pp. 127-141.

22. Gunter, E. J., Barrett, L. E., and Allaire, P. E., "Balancing of Multimass Flexible Rotors, Part I: Theory," Proceedings of the Fifth Turbomachinery Symposium, Texas A & M University Press, Oct. 1976, pp. 133-147.

23. Gunter, E. J., Barrett, L. E., and Allaire, P. E., "Balancing of Multimass Flexible Rotors, Part II: Experimental Results," Proceedings of the Fifth Turbomachinery Symposium, Texas A & M University Press, Oct. 1976.

24. Gunter, E. J., Choy, K. C., and Allaire, P. E., "Modal Analysis of Turborotors Using Planar Modes - Theory," Journal of the Franklin Institute, Vol. 305, No. 4, 1978, pp. 221-243.

25. Gunter, E. J., Li, D. F., and Barrett, L. E., "A Dymamic Analysis of Multispool Gas Turbine Helicopter Engine," Proceedings of the Conference on Stability and Dynamic Response of Rotors in Squeeze Film Bearings, U.S. Army Research and Development Laboratory, Washington, D.C., 1979.

26. Gunter, E. J., Springer, H., and Humphris, R. R., "Balancing of a Multimass Flexible Rotor-Bearing System Without Phase Measurements," Conference on Rotordynamics Problems in Power Plants, Rome, Italy, Sept. 1982.

27. Hassenpflug, H. L., Flack, R. D., and Gunter, E. J., "Influence of Acceleration on the Critical Speed of a Jeffcott Rotor," ASME Paper No. 80-GT-88, Journal of Engineering for Power, TRANS. ASME, May 1980.

28. Hassenpflug, H. L., Flack, R. D., and Gunter, E. J., "Experimental Study of the Critical Speed Response of a Jeffcott Rotor With Acceleration," Journal of the Franklin Institute, Vol. 310, No. 1, July 1980, pp. 77-88.

29. Hori, Y., "A Theory of Oil Whip," Journal of Applied Mechanics, TRANS. ASME, June 1959, pp. 189-198.

30. Kirk, R. G., and Gunter, E. J., "Transient Journal Bearing Analysis," NASA Contract Report, Federal Scientific and Technical Information, Springfield, Virginia, NASA CR-1549, June 1970.

31. Kirk, R. G., and Gunter, E. J., "Nonlinear Transient Analysis of Multi-Mass Flexible Rotors - Theory and Applications," NASA CR-2300, Washington, D.C., Sept. 1973.

32. Kirk, R. G., De Choudhury, P., and Gunter, E. J., "The Effect of Support Flexibility on the Stability of Rotors Mounted in Plain Cylindrical Journal Bearings," Dynamics of Rotors, Springer-Verlag, New York, 1975, pp. 244-298.

33. Kirk, R. G., and Gunter, E. J., "Stability and Transient Motion of a Plain Journal Mounted in Flexible Damped Supports," Journal of Engineering for Industry, TRANS. ASME, Vol. 98, Series B, No. 2, May 1976, pp. 576-592.

34. Kirk, R. G., and Gunter, E. J., "Short Bearing Analysis Applied to Rotor Dynamics, Part I: Theory," Journal of Lubrication Technology, TRANS. ASME, Vol. 98, Series F, No. 1, Jan. 1976, pp. 47-56.

35. Kirk, R. G., and Gunter, E. J., "Short Bearing Analysis Applied to Rotor Dynamics, Part II: Results of Journal Bearing Response," Journal of Lubrication Technology, TRANS. ASME, Vol. 98, No. 2, Apr. 1976, pp. 319-329.

36. Leader, M. E., Flack, R. D., and Lewis, D. W., "An Experimental Determination of the Instability of a Flexible Rotor in Four-Lobe Bearings," Wear, Vol. 58, No. 1, Jan. 1980, pp. 35-47.

37. Lee, C. C., Allaire, P. E., and Simpson, M. A., "Dynamic Analysis of a Short Journal Bearing," International Journal of Mechanical Engineering Education, Vol. 6, No. 4, Dec. 1978, pp. 175-179.

38. Li, D. F., Allaire, P. E., and Barrett, L. E., "Analytical Dynamics of Partial Journal Bearings with Applications," Transactions of the American Society of Lubrication Engineers, Vol. 22, No. 2, Apr. 1979, pp. 99-112.

39. Li, D. F., and Gunter, E. J., "Component Mode Synthesis of Large Rotor Systems," ASME Paper 81-GT-147, ASME Gas Turbine Conference, Journal of Engineering for Power, TRANS. ASME, Mar. 1981.

40. Li, D. F., and Gunter, E. J., "A Study of the Modal Truncation Error in the Component Mode Analysis of a Dual-Rotor System," ASME Paper 81-GT-144, Journal of Engineering for Power, TRANS. ASME, Mar. 1981.

41. Lund, J. W., and Orcutt, F. K., "Calculations and Experiments on the Unbalance Response of a Flexible Rotor," Journal of Engineering for Industry, TRANS. ASME, Vol. 89, Series B, No. 4, Nov. 1967, pp. 785-796.

42. Lund, J. W., and Saibel, E., "Oil Whip Whirl Orbits of a Rotor in Sleeve Bearings," Journal of Engineering for Industry, TRANS. ASME, Vol. 89, Series B, No. 4, Nov. 1967, pp. 813-823.

43. Lund, J. W., and Thomsen, K. K., "A Calculation Method and Data for the Dynamic Coefficients of Oil-Lubricated Journal Bearings," ASME Topics in Fluid Film Bearings and Rotor-Bearing System Design and Optimization, Apr. 1978, pp. 1-28.

44. Nelson, H. D., and Meacham, W. L., "Transient Analysis of Rotor-Bearing Systems Using Component Mode Synthesis," ASME Paper 81-GT-110, Gas Turbine Conference, Mar. 1981.

45. Pilkey, W. D., Chang, P. Y., and Strendowski, J., "General Modal Transient Response of Rotating Shafts," Journal of Engineering for Industry, TRANS. ASME, 1978.

46. Ruhl, B. L., and Booker, J. F., "A Finite Element Model for Distributed Parameter Turbomotor Systems," Presented at the ASME Vibration Conference, ASME Paper 71-VIBR-56, 1971.

47. Salamone, D. J., and Gunter, E. J., "Effects of Shaft Warp and Disc Skew on the Synchronous Unbalance Response of a Multimass Rotor in Fluid Film Bearings," ASME Proceedings, Topics in Fluid Film Bearing Design and Optimization, Apr. 1978, pp. 79-107.

48. Salamone, D. J., Gunter, E. J., and Barrett, L. E., "Balancing of a Double Overhung Compressor with Skewed Wheels and a Bowed Shaft," I. Mech. E., Proceedings of the Second International Conference on Vibrations in Rotating Machinery, Cambridge, England, Sept. 1980.

49. Salamone, D. J., and Gunter, E. J., "Synchronous Unbalance Response of an Overhung Rotor with Disc Skew," Journal of Engineering for Power, TRANS. ASME, Vol. 102, Oct. 1980, pp. 749-755.

50. Simpson, M. A., and Barrett, L. E., "Suppression of Self-Excited Instability Using a Squeeze Film Bearing," Proceedings of the Conference on the Stability and Dynamic Response of Rotors with Squeeze Film Bearings, Research Triangle Park, North Carolina, May 1979, pp. 24-52.

51. Springer, H., "Nichtlineare Schwingungen schwerer Rotoren mit vertikaler Welle und Kippsegmentradiallagern. Forschg. Ing. Wesen 45, 1979, pp. 119-132.

52. Tondl, A., "On the Interaction Between Self-Excited and Forced Vibrations," National Research Institute for Machine Design, Monographs and Memoranda No. 20, Prague, 1976, pp. 144-171.

53. Woomer, E., and Pilkey, W. D., "The Balancing of Rotating Shafts by Quadratic Programming," Journal of Mechanical Design, 1980.

54. Zorzi, E. S., and Nelson, L. D., "Finite Element Simulation of Rotor-Bearing Systems with Internal Damping," Journal of Engineering for Industry, TRANS. ASME, Vol. 99, No. 1, Jan. 1977, pp. 71-76.

ACKNOWLEDGEMENTS

This research has been supported by NASA and the industrially supported Turbomachinery Dynamics Research Program, Rotor Dynamics Laboratory, University of Virginia. Particular acknowledgement is also given to Centritech Corp. for providing the test rig and to the Bently Nevada Corp. for the equipment and test rigs provided to the Rotor Dynamics Laboratory. Acknowledgement is also expressed to the Bently Nevada Corp. for the use of the ADRE software used in generating many of the experimental curves. Acknowledgement is also extended to the various faculty members and students who have participated in the research program at the Rotor Dynamics Laboratory at the University of Virginia.